6.4 TURBULENT AND RADIATIVE STRUCTURE OF ALTOCUMULUS CLOUDS

Vincent E. Larson[1] *, Christopher M. Sears[1] , Jean-Christophe Golaz[2]
[1] Dept. of Mathematical Sciences, University of Wisconsin — Milwaukee, Milwaukee, Wisconsin.
[2] Dept. of Atmospheric Science, Colorado State University, Fort Collins, Colorado.

1. INTRODUCTION

Altocumulus clouds are thin layer clouds that exist in the mid levels of the troposphere and contain turbulent cloud elements.

There are several motivations to study altocumulus clouds. Perhaps foremost is a scientific motivation: altocumulus clouds provide a simple laboratory in which to study the general nature and interaction of latent heating, radiation, and turbulence. There are also practical motivations. First, mid level clouds often contain supercooled water, which can be an icing hazard (Cober et al. 2001). Second, mid level clouds contain horizontal variability in water content that, if ignored, may lead to a bias in the calculation of radiative emissivity (Pomroy and Illingworth 2000; Garrett et al. 2002). Third, large-scale models tend to underpredict the presence of mid level clouds (Ryan et al. 2000).

In this paper, we perform idealized large eddy simulations of an altocumulus cloud that was observed by aircraft during the Complex Layered-Cloud Experiment 5 (CLEX-5) field experiment on 11 Nov 99 (Larson et al. 2001; Fleishauer et al. 2002). The cloud occurred over Montana U.S.A. and was about 500 m thick at the beginning of the measurement period. The cloud was overcast and mixed phase but contained little ice or precipitation.

The aspect of this cloud that we focus on is the interaction of radiation, turbulence, and entrainment. Radiative cooling at cloud top generates descending plumes. These plumes extend below cloud base. Thus the turbulently mixed layer is greater in depth than the cloud layer. The depth of the turbulently mixed layer is expected to affect the evolution of the liquid water path in such clouds via entrainment or detrainment of air from above or below cloud.

2. MODEL DESCRIPTION

The set up of the control simulation is as follows. The model used was RAMS version 4.3 (Cotton et al. 2002). All precipitation and ice processes in the simulation were turned off in order to focus on the interaction of radiation, turbulence, and entrainment. The control simulation ignored shortwave radiation but did compute longwave radiation using the two-stream scheme of Harrington et al. (1999). The model domain included the cloud at midlevels and extended to the ground (at approximately 1100 m MSL). The simulation had a horizontal domain size of 4 km $\times$ 4 km and a vertical domain size of 6.75 km. The corresponding grid spacing was 50 m $\times$ 50 m $\times$ 25 m. The initial profiles of the conserved variables total water mixing ratio, r_t, and liquid water potential temperature, θ_l, were horizontally homogeneous idealizations of profiles observed during the 11 Nov 99 case. We used two sources of data: a spiral aircraft sounding at 1930 UTC that extended from about 100 m above cloud to 300 m below cloud, and a radiosonde profile that was obtained at Great Falls, MT (station TFX) at 0 UTC on 12 Nov 99, about 175 km west of and 4.5 hours after the aircraft sounding.

*Corresponding author address: Vincent E. Larson, Department of Mathematical Sciences, University of Wisconsin — Milwaukee, P. O. Box 413, Milwaukee, WI 53201-0413; e-mail: vlarson@uwm.edu

3. CLOUD STRUCTURE

The simulation was initiated at 1730 UTC, and the turbulence was allowed to spin up for two hours. The profiles at the end of the spinup time are shown in Fig. 1.

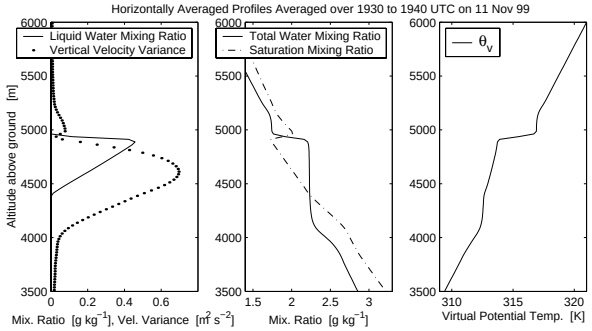

Figure 1: Simulated profiles averaged from 1930 to 1940 UTC, after 2 hours of spinup time. This time corresponds approximately to the time of the aircraft sounding.

The simulated liquid water increases with increasing altitude. The profile approximates the observed one, except that the simulated cloud is 350 m higher in altitude, mostly because of upward growth of the cloud layer during the spinup period. The model creates a well-mixed turbulent layer that extends throughout the cloud layer and about 350 m below cloud base. The observed layer was not as well mixed in r_t and θ_l. The aircraft sounding also has smaller jumps at the above-cloud inversion ($\Delta r_t \cong -0.35$ g kg^{-1} and $\Delta\theta_v \cong 1$ K) than the simulation ($\Delta r_t = -0.5$ g kg^{-1} and $\Delta\theta_v = 3$ K). Here θ_v denotes the virtual potential temperature. The within-cloud turbulence, as measured by the variance of vertical velocity, is

similar in magnitude ($\overline{w'^2} \sim 0.5$ m^2 s^{-2}) in the simulation and observations.

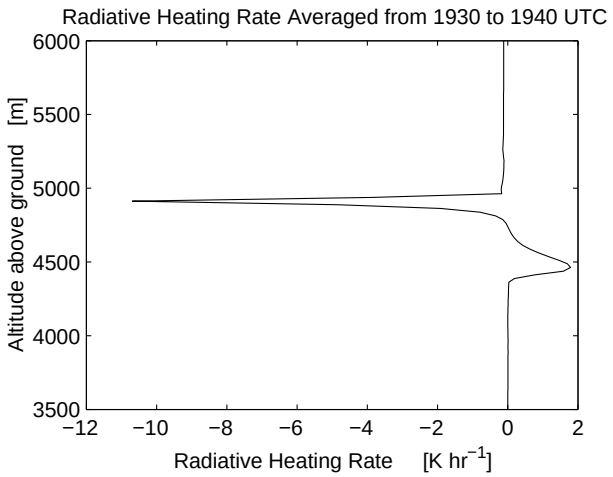

Figure 2: Simulated profile of radiative heating rate averaged from 1930 to 1940 UTC, after 2 hours of spinup time. This time corresponds approximately to the time of the aircraft sounding.

The turbulence in the model is not generated by instability and breakdown of vertical wind shear, since no shear was imposed in the model. Rather, radiative cooling occurs at cloud top, and radiative warming occurs at cloud base (Fig. 2). The profile of radiative cooling is qualitatively similar to that found in stratocumulus, except that the altocumulus cloud has significant cloud base warming because the ground is significantly warmer than cloud base. The differential radiative heating leads to buoyant instability, that is, dense air above light air. Radiatively cooled parcels descend from cloud top, generating turbulence. However, the plumes do not stop their descent at cloud base. Instead, the radiatively cooled parcels penetrate several hundred meters below cloud base. This simplified picture of turbulence generation may be modified by entrainment at the boundaries of the mixed layer.

The extent of the mixed layer below cloud base is important for the time evolution of the cloud liquid water. Altocumulus clouds like the 11 Nov 99 case may be modeled using an elevated mixed layer model (Lilly 1988; Liu and Krueger 1998). The values of r_t and θ_l within the turbulent well-mixed layer change because of net radiative cooling within the layer and because of entrainment into the top and bottom of the mixed layer. The rapidity with which these forcings alter r_t and θ_l depends on the depth of mixed layer, with deeper layers suffering less change.

The nature of the turbulence is illuminated by the budget of horizontally averaged turbulent kinetic energy (TKE) shown in Fig. 3. In this calculation, the time rate of change of TKE has been assumed to be negligible, and the viscous dissipation term has been computed as a residual of the other terms. Within the cloud layer, the

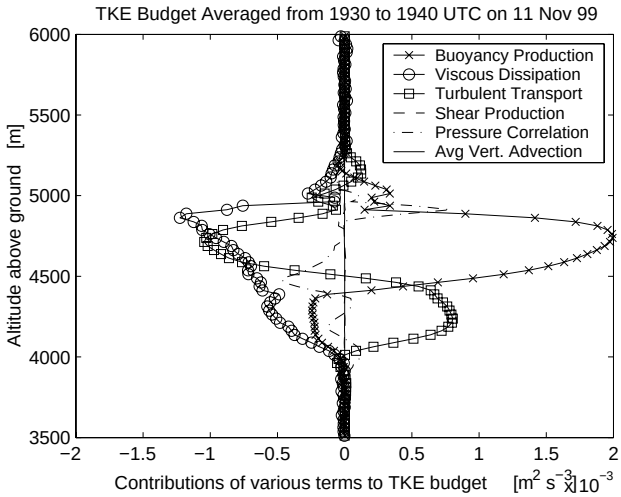

Figure 3: Simulated profiles of terms in TKE budget averaged from 1930 to 1940 UTC, after 2 hours of spinup time. This time corresponds approximately to the time of the aircraft sounding of the 11 Nov 99 field experiment.

major source of TKE is buoyant production, and the major sinks of TKE are viscous dissipation and turbulent transport. Buoyancy generates TKE if $\overline{w'\theta'_v} > 0$, that is, if cool parcels descend and warm parcels ascend. The positive buoyancy production is ultimately caused by the differential radiative heating across the layer. Below the cloud layer, the major source of TKE is turbulent transport, and the major sinks are viscous dissipation and buoyancy production. Below cloud base, buoyancy production is negative, that is, warm parcels descend, thereby consuming TKE. TKE is maintained below cloud only because it is advected there from the cloud layer. In summary, the turbulence below cloud base consists of descending plumes that undershoot their level of neutral buoyancy.

The extent of the undershooting is difficult to predict. Liu and Krueger (1998) estimated the below-cloud mixed-layer depth by assuming that the integrated negative buoyancy production below cloud base is a fixed fraction of the integrated positive buoyancy production within the cloud layer. The rationale is that a fixed fraction of the turbulence generated in cloud is transported below cloud. Numerically, the simulations of Liu and Krueger (1998) for clouds with small liquid water path find that

$$\frac{\int_{\text{mixed-layer base}}^{\text{cloud base}} \overline{w'\theta'_v}\, dz}{\int_{\text{cloud base}}^{\text{cloud top}} \overline{w'\theta'_v}\, dz} \cong -0.02.$$

The simulation for the 11 Nov 99 case finds a value of about -0.1, which has a magnitude about 5 times larger than Liu and Krueger's cases.

More can be learned about the descending plumes by examining their joint probability density functions (PDFs), displayed in Figs. 4 and 5. The below-cloud PDFs have a long tail corresponding to negative velocities, i.e. downdrafts. The values of the conserved variables r_t and θ_l

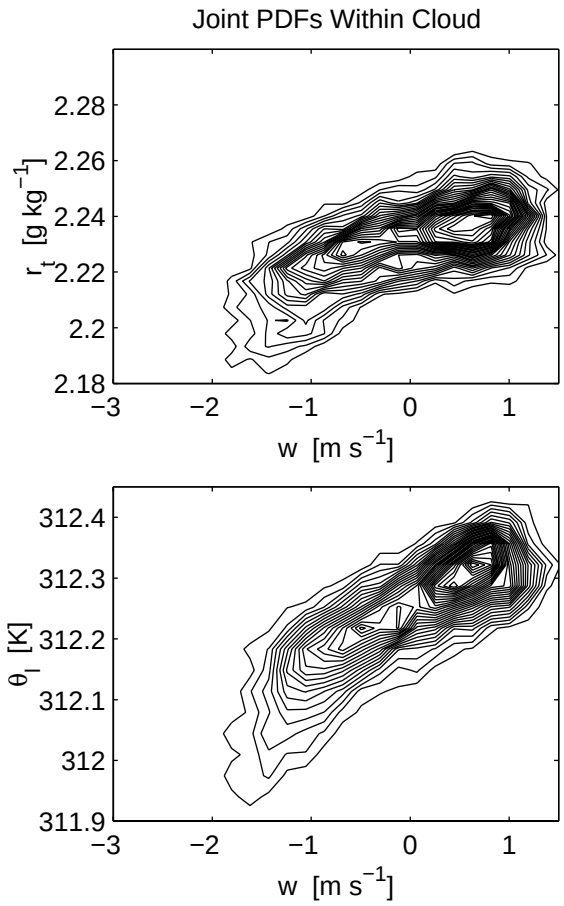

Figure 4: Joint PDFs within cloud averaged over a horizontal layer at $z = 4713$ m and 1930 UTC. $\overline{r_l} = 0.3$ g kg^{-1}. Skewness of $w = \overline{w'^3}/(\overline{w'^2})^{1.5} = -0.39$; skewness of $r_t = \overline{r_t'^3}/(\overline{r_t'^2})^{1.5} = -0.70$; skewness of $\theta_l = \overline{\theta_l'^3}/(\overline{\theta_l'^2})^{1.5} = -0.97$.

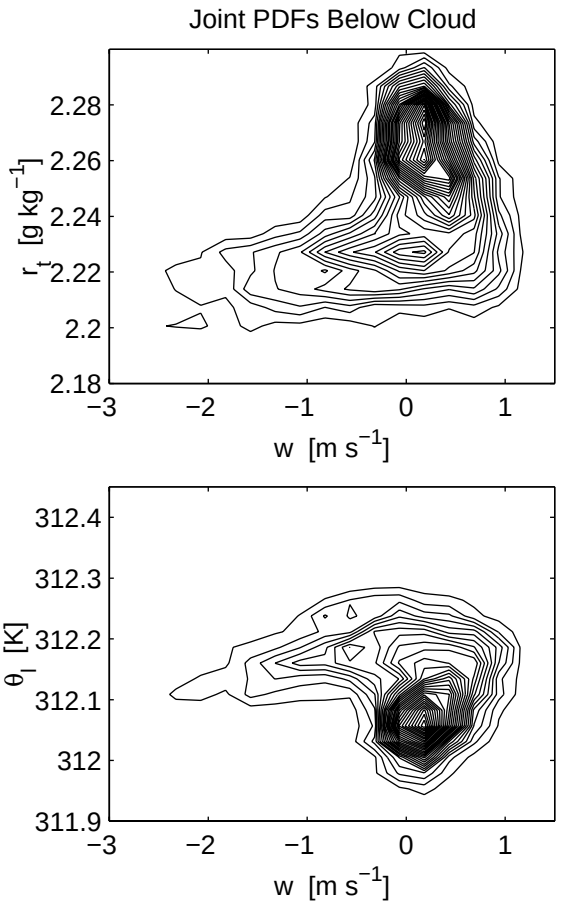

Figure 5: Joint PDFs in the well-mixed layer below cloud averaged over a horizontal layer at $z = 4263$ m and 1930 UTC. $\overline{r_l} = 0.0$ g kg^{-1}. Skewness of $w = \overline{w'^3}/(\overline{w'^2})^{1.5} = -1.7$; skewness of $r_t = \overline{r_t'^3}/(\overline{r_t'^2})^{1.5} = 0.0$; skewness of $\theta_l = \overline{\theta_l'^3}/(\overline{\theta_l'^2})^{1.5} = 0.0$.

in the below-cloud downdrafts are similar to those for the within-cloud downdrafts. However, the values of r_t and θ_l in the environment, i.e. the region with small or positive velocity, change with altitude. This hints that the plumes are coherent structures that carry conserved scalars from mid cloud to below cloud without much mixing, even though the surrounding environment changes with altitude.

4. CLOUD EVOLUTION

Net radiative cooling throughout the cloud layer tends to increase liquid water. However, differential radiative heating generates turbulence, which may dry out the cloud by entraining dry air from above the cloud. In addition, if entrainment increases cloud top height, the resulting adiabatic cooling would tend to increase liquid water (Randall 1984). Given the uncertainty in the measurements of Larson et al. (2001), it is unclear for the 11 Nov 99 case whether the net effect of radiation and the concomitant entrainment was to enhance or deplete the liquid water.

In nature, the evolution of liquid water is complicated by the presence of large-scale subsidence and precipitation. However, the numerical model can isolate the effect of radiation and entrainment by setting subsidence and precipitation to zero. The resulting time evolution of the liquid and total water profiles is illustrated in Fig. 6.

We see that both cloud top and cloud base rise, but cloud top rises faster, leading to an increase of liquid water path with time. This is perhaps somewhat counterintuitive, since the 11 Nov 99 cloud is clearly dynamically decoupled from the surface, and decoupling is thought to be the first stage in the breakup of boundary layer stratocumulus into cumulus clouds.

Although the cloud base rises, the base of the turbulent mixed layer descends, as the turbulent plumes penetrate downward. Liu and Krueger (1998) found in their

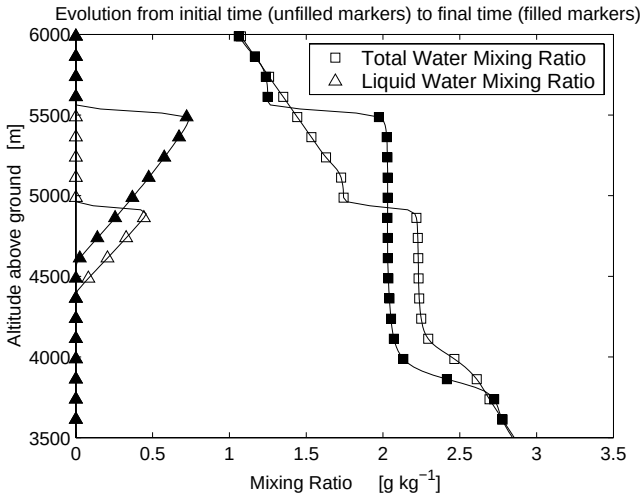

Figure 6: Liquid water and total water (liquid + vapor) horizontally averaged profiles from the control simulation. The initial profiles are averaged from 1930 to 1940 UTC 11 Nov 99; the final profiles are averaged from 0220 to 0230 UTC 12 Nov 99.

cases that the base of the turbulently mixed layer usually ascended. Whether the mixed layer ascends or descends is important because if the cloud base descends, air is entrained into the layer from below, thereby moistening it. This process is less important for decoupled marine stratocumulus clouds, which usually do not have a strong vertical gradient of r_t beneath them.

The increase in liquid water path found in the simulations disagrees with the observed dissipation of the 11 Nov 99 cloud after 74 minutes (Larson et al. 2001). This hints that one or more processes that dissipated the observed cloud were ignored in the simulation. To investigate one aspect of this, we performed a simulation that was identical to the control simulation except that solar radiation was turned on. The solar angle was calculated based on the location of the observed cloud (Montana, U.S.A.), its date (11 Nov 99), and time of day (1930 UTC). Solar absorption decreased the liquid water path by up to 30% but did not cause the cloud to disappear. The most obvious remaining culprits for the disappearance of the cloud are large-scale subsidence and precipitation.

5. CONCLUSIONS

We have performed a large eddy simulation of an altocumulus cloud that was observed during the CLEX-5 field campaign. In the simulation, radiative cooling generates turbulent plumes that undershoot their level of neutral buoyancy and thereby extend below cloud base. The depth of the turbulent layer below cloud is difficult to predict using the standard methodology. The depth is important, however, because it affects the time evolution of the cloud layer. Because moisture is vertically stratified below cloud, entrainment of air from below can moisten the cloud layer. This stratification below cloud is different than that for marine stratocumulus layers. Finally, the net effect of radiation and entrainment in the simulation is to increase liquid water path.

Acknowledgements V. E. Larson gratefully acknowledges support from subawards G-7420-2 and G-7470-2 from the Center for Geosciences at Colorado State University. Jean-Christophe Golaz acknowledges support from the National Science Foundation under grant ATM-9904218.

6. REFERENCES

Cober, S. G., G. A. Isaac, and J. W. Strapp, 2001: Characterizations of aircraft icing environments that include supercooled large drops. *Journal of Applied Meteorology*, **40**, 19842002.

Cotton, W. R., R. A. Pielke Sr., R. L. Walko, G. E. Liston, C. J. Tremback, H. Jiang, R. L. McAnelly, J. Y. Harrington, and M. E. Nicholls, 2002: Rams 2001: Current status and future directions. Accepted to Meteorology and Atmospheric Physics.

Fleishauer, R. P., V. E. Larson, and T. H. Vonder Haar, 2001: Observed microphysical structure of midlevel, mixed-phase clouds. *J. Atmos. Sci.*, **59**, 1779–1804.

Garrett T.J., L. F. Radke, and P. V. Hobbs, 2002: Aerosol effects on cloud emissivity and surface longwave heating in the arctic. *J. Atmos. Sci.*, **59**, 769–778.

Harrington, J. Y., T. Reisin, W. R. Cotton, and S. M. Kreidenweis, 1999: Cloud resolving simulations of arctic stratus. Part II: Transition-season clouds, *Atmos. Res.*, **51**, 4575.

Larson, V. E., R. P. Fleishauer, J. A. Kankiewicz, D. L. Reinke, and T. H. Vonder Haar, 2001: The Death of an Altocumulus Cloud. *Geophys. Res. Lett.*, **28**, 2609-2612.

Lilly, D. K., 1988: Cirrus outflow dynamics. *J. Atmos. Sci.*, **45**, 1594–1605.

Liu, S. and Krueger, S. K., 1998: Numerical Simulations of Altocumulus Using a Cloud Resolving Model and a Mixed Layer Model. *Atmos. Res.*, **47-48**, 461-474.

Pomroy H.R., and A. J. Illingworth, 2000: Ice cloud inhomogeneity: Quantifying bias in emissivity from radar observations. *Geophys. Res. Lett.*, **27**, 2101-2104.

Randall, D. A., 1984: Stratocumulus cloud deepening through entrainment. *Tellus*, **36A**, 446–457.

Ryan, B. F., and Coauthors, 2000: Simulations of a cold front by cloud-resolving, limited-area, and large-scale models, and a model evaluation using in situ and satellite observations. *Mon. Wea. Rev.*, **128**, 32183235.